Convection in a long vertical tube due to unstable stratification – A new type of turbulent flow?

Jaywant H. Arakeri*,§, Fransisco E. Avila†, Jorge M. Dada and Ramon O. Tovar

*Department of Mechanical Engineering, Indian Institute of Science, Bangalore 560 012, India
Centro De Investigacion en Energia, Temixco, UNAM, Mexico

We present experimental results of free convection in a vertical tube due to an unstable density difference imposed between the two (open) ends of the tube. Two tanks of fluids connect the two ends of the tube with the top-tank fluid heavier than the bottom-tank fluid. We use salt mixed with water to create the density difference. The convection in the tube is in the form of relatively heavier fluid going down and lighter fluid going up simultaneously; the mean flow at any cross section of the tube is zero. Depending on the Rayleigh number we observe different types of flow, with turbulent flow being observed at the higher Rayleigh numbers. We believe this is a new type of turbulent flow – a nearly homogeneous, buoyancy-driven flow with zero mean shear.

FLOWS caused by buoyancy, called free or natural convection, abound in nature and engineering. The convection observed on a hot road surface in no-wind conditions is an example. Convection is generally caused by unstable stratification (for example, density increasing with height in a gravitational field). Density gradients are often caused by a temperature gradient, or a gradient of concentration of some species (e.g. salt in the oceans, water vapour in air). The dynamics in free-convection flows is mainly determined by the Rayleigh number – a measure of the ratio of buoyancy forces to diffusive effects.

Two simple configurations of free convection have been extensively studied, viz. Rayleigh–Benard convection and Rayleigh–Taylor instability. Rayleigh–Benard (R–B) convection is convection of a fluid between two horizontal plates, with the bottom plate hotter than the top plate. Because of the temperature difference, the fluid density increases from the bottom plate to the top plate. However, below a critical Rayleigh number, even though the stratification is unstable, there is no flow (convection) and heat transfer is entirely by conduction; the Rayleigh number increased beyond this critical value results in laminar convection, often in the form of rolls, and a further increase in the Rayleigh number leads to turbulent convection (see ref. 1).

§For correspondence. (e-mail: jaywant@mecheng.iisc.ernet.in)
†Sadly, Fransisco passed away during the writing of this paper. We have fond memories of him.

Rayleigh–Taylor instability occurs when a layer of heavier fluid (say salt water) lies on top of a layer of lighter fluid (say fresh water). Dalziel *et al.*[2] report recent work on this subject. In this configuration the layers can be in equilibrium; pressure varies linearly with depth in each of the layers. But this is unstable equilibrium: a small perturbation of the interface increases the perturbation indefinitely with the heavier fluid trying to go down and the lighter fluid trying to go up. Some mixing between the top and bottom fluids occurs during the overturning. Eventually motion ceases and a stable density gradient is obtained. For an immiscible pair of fluids of say water over air there is negligible mixing and, eventually, the water and air layers just interchange places. One common way of doing a Rayleigh–Taylor stability experiment is to have a thin plate initially separating the two fluids which is then rapidly pulled away.

In this article we describe preliminary results of free convection in a vertical tube. The setup is similar to a Rayleigh–Taylor stability setup, except that we have a long vertical tube between the tanks containing the heavier fluid at the top and the lighter fluid at the bottom (Figure 1). So essentially we look at the 'overturning' process of the two fluids through the tube. We used sodium chloride salt mixed in water to create the density difference. As in Rayleigh–Benard convection, we find different types of flow depending on the values of the parameters of the problem: the density difference, and diameter and length of the tube. In particular, at a high enough Rayleigh number we observe the flow to be turbulent, which we believe is a new type of turbulent flow.

Experimental setup

The experimental setup consisted of two tanks connected by a vertical tube. The top tank was open at the top and had a tapered hole in the bottom plexiglas wall to fit a rubber stopper; an appropriate sized hole was made in the stopper to snugly fit the tube. The bottom tank was closed on all sides and had a similar rubber stopper arrangement on the top wall to fit the bottom end of the tube. The rubber stoppers minimized the load

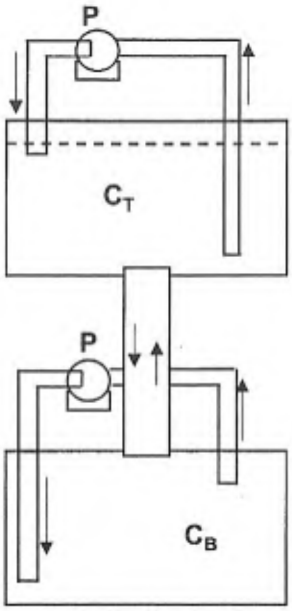

Figure 1. Schematic of the experimental setup. The pumps in the two tanks are marked P.

on the tubes, which were made of glass, and also allowed us to quickly change the tube for a different experiment. The side walls of the tanks were made of glass. Two small aquarium water pumps were used to continuously mix the fluids in the two tanks and prevent stratification. The flow rates in the pumps were small enough and the locations of the exits and inlets of the pumps were such as to create as small a disturbance as possible near the tube ends.

The volumes of the two tanks were approximately 1750 cc each. A total of twelve tubes were used in the experiments, with four diameters (4.85, 9.85, 19.85 and 36.85 mm) and three lengths (150, 300 and 450 mm). A few visualization experiments were conducted with 2.5 mm diameter tubes.

Following is the experimental procedure. We calibrated the conductivity probes, used to measure salt concentration, before and after each experiment. We filled the bottom tank and the tube with distilled water, and the top tank with brine (typically 0.05 g cm^{-3} concentration), noting down the volumes of the distilled water and brine added. We switched on the pumps prior to the start of each experiment. Initially, a stopper blocked the top end of the tube; pulling of the stopper initiated the experiment. Due to the convection the salt concentration in the top tank continuously decreased with time (Figure 2). Concentration in the top tank was measured from the start of the experiment till the convection had visibly stopped. In the smallest diameter and longest tube (4.85 mm dia, 600 mm long) the convection continued for about 100 h, whereas in the largest diameter tube the convection continued for about 1 h.

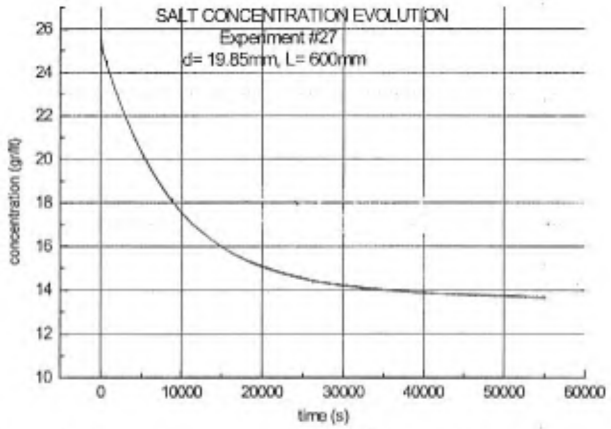

Figure 2. A typical variation of concentration of salt in the top-tank fluid with time. The case shown corresponds to tube diameter = 19.85 mm and tube length = 600 mm.

Salt concentration was measured with one or two micro-conductivity probes (Model 125 MSCTI, Precision Measurements Engineering), placed in the top tank. The concentration versus time data were stored in a computer for further analysis. Two conductivity probes were used to check that mixing by the pump was adequate and there was no concentration gradient in the tank fluid. We mainly visualized the flow using the laser-induced-fluorescence (LIF) technique. A small amount of sodium fluorescent dye was initially mixed in the top tank fluid. A vertical sheet of laser light, created with a cylindrical lens, passed through the vertical tube (in which the convection was taking place). We used a 150 mW argon-ion laser. In some cases, we also visualized the flow using the shadowgraph technique.

Parameters

We are looking at free convection in a vertical tube open at the two ends, with an imposed density, or concentration, difference across it. As in Rayleigh–Benard convection, the non-dimensional parameters of the problem are:

$$\text{Rayleigh number, } \mathrm{Ra}_l = \frac{g\Delta C l^3}{\rho\nu\alpha},$$

$$\text{Prandtl number, } \mathrm{Pr} = \frac{\nu}{\alpha},$$

$$\text{Aspect ratio, } \mathrm{AR} = \frac{d}{l},$$

where ΔC is the concentration (or density) difference between the top tank and bottom tank fluids, ρ, is the density of the fluid averaged over the length of the tube, g is acceleration due to gravity, ν is the kinematic viscosity, α is the diffusivity of the species causing

the density gradient, d is tube diameter, and l is tube length.

Sometimes it is more appropriate to use other definitions of Rayleigh number: Ra_d, Rayleigh number based on the tube diameter, and Ra_G, Rayleigh number based on the density gradient, instead of density difference, and diameter.

Some values of the parameters are of interest. The Prandtl number, or strictly the Schmidt number, is about 670, showing diffusion of salt is negligible in comparison to that of momentum. At a concentration difference of 0.025 g/cm^3 and for a tube length = 600 mm, the Rayleigh number = 3.5×10^{13}. The AR ranges from about 0.008 to about 0.25. For comparison, study of turbulent Rayleigh–Benard thermal convection is usually with Pr ~ 1 (for air Pr = 0.7 and for water Pr = 6.7); the Rayleigh number is usually of the order of 1×10^8, but the highest value achieved, reported recently[3], using cryogenic helium is about 1×10^{17}; and AR is usually greater than unity. Thus the present problem pertains to very large Rayleigh number, high Prandtl number convection in tall cells. High Prandtl number, high Rayleigh number convection is generally obtained with very viscous fluids convecting over a large scale, as in convection in the earth's mantle.

Basic relations

From the salt concentration (in the top tank) versus time data we calculate the flux of salt, and the concentration difference between the two tank fluids as functions of time. This is done using mass conservation equations.

We use cylindrical polar coordinates (r, θ and z) with velocities in the three directions respectively, U_r, U_θ and W. The z-axis coincides with tube axis and is positive upwards. An overbar over a quantity denotes the quantity averaged over the cross-section of the tube. The difference between a quantity and its average is written in small case. Thus for concentration

$$\overline{C} = \int_A C \mathrm{d}A, \quad c = C - \overline{C}.$$

Fluid volumes in each of the two tanks do not change with time. Thus, at any cross-section of the tube and any instant of time (assuming water to be incompressible) the volume flow rate of the fluid going down = the volume flow rate of fluid going up, or

$$\int_A W \mathrm{d}A = \overline{W} = 0.$$

We come to the important conclusion that the mean velocity at any cross-section is zero.

The mass flow rate of salt $\dot{m}_s$ going up at any z is

$$\dot{m}_s = \int_A CW \mathrm{d}A = \overline{cw} A_p,$$

where A_p is the cross-sectional area of the tube. From mass conservation of salt at any z we have the gradient of $\dot{m}_s$,

$$\frac{\partial \dot{m}_s}{\partial z} = -\frac{\partial}{\partial t}\left(\int_A (C \mathrm{d}A)\right) = -A_p \frac{\partial \overline{C}}{\partial t}.$$

The equation states that in a control volume height dz, the difference in mass flow rates at two stations dz apart is equal to the rate at which mass of salt changes in the control volume. If $(\partial \overline{C}/\partial t) = 0$, then $\dot{m}_s$ is constant along the length of the tube; however, $\dot{m}_s$ can still be a function of time.

At any time let C_T and C_B be the concentrations of salt in the top and bottom tanks respectively, and C_{T0} and C_{B0} the concentrations at the start of the experiment. Mass conservation of salt gives

$$V_T C_T + V_B C_B + A_p \int_0^l \overline{C} \mathrm{d}z = V_T C_{T0} + V_B C_{B0} + A_p \int_0^l \overline{C}_0 \mathrm{d}z = M_s,$$

Where V_T and V_B are respectively the top and bottom tank fluid volumes, A_P is the pipe cross section area, and M_s is the total mass of salt in the system. The integral on the left-hand side is the mass of the salt in the tube. Assuming the average salt concentration in the tube at any time is $(C_T + C_B)/2$, we obtain the following relation for the concentration or density difference in terms of the concentration in the top tank:

$$\Delta C = (C_T - C_B) = C_T \frac{(V_T + V_B + V_P)}{(V_B + V_P/2)} - \frac{M_s}{(V_B + V_P/2)}, \quad (1)$$

where V_p is the volume of the tube.

Let $\dot{m}_{sT}$ be mass flow rate of salt at the top end of the tube and $\dot{m}_{sB}$ at the bottom end of the tube. Then

$$\dot{m}_{sT} = V_T \mathrm{d}C_T/\mathrm{d}t, \quad \dot{m}_{sB} = -V_B \frac{\mathrm{d}C_B}{\mathrm{d}t},$$

$$\dot{m}_{sT} - \dot{m}_{sB} = \frac{\mathrm{d}}{\mathrm{d}t}\int_0^l \overline{C} \mathrm{d}z.$$

The relations respectively are from salt mass conservation in the top tank, bottom tank and in the tube. In

our experiments, to a good approximation, we can assume

$$\dot{m}_{sT} = \dot{m}_{sB} = \dot{m}_s = V_T \frac{dC_T}{dt}.$$

Then flux, mass flow rate of salt going down per unit cross sectional area of the tube is,

$$F = -\overline{cw} = -\frac{V_T}{A_p}\frac{dC_T}{dt}. \quad (2)$$

Flow visualization observations

Depending on the concentration difference, the tube diameter and the tube length we observe one of four types of flow which we term (i) half-and-half (HAH), (ii) helical, (iii) unsteady-laminar and (iv) turbulent. These are described below. It may be noted that the flow visualization pictures given in this paper show just a few centimetres length of the central portion of the tube.

Half-and-half flow

In a HAH flow, in one half of the cross section of the tube flow is downward, and in the other half the flow is upward. We observed the HAH flow only in the 2.5 mm dia tube and in the 4.85 mm dia tube at small concentration differences, essentially meaning at low Rayleigh numbers. In some cases we observed moving fronts, about 1–2 tube diameters long. A downward moving front is heavier and moves faster than the rest of the down-going fluid; similarly an upmoving front is lighter than the rest of the up-going fluid. Figure 3 is a shadowgraph picture showing both down-going and up-going fronts.

Figure 3. Shadowgraph picture showing two fronts in HAH convection. Tube diameter is 2.5 mm.

Figure 4. LIF picture showing helical convection. Tube diameter = 4.8 mm; tube length = 150 mm; concentration difference = 0.025 g/cc. Top-tank fluid is dyed. Only the central length of the tube is shown.

Helical flow

We observed helical flow in the 4.85 mm dia tube (Figure 4), except at small concentration differences when the flow was HAH (Figure 4). As in HAH flow the helical flow is equally divided between up-going and down-going fluid, and is steady. In HAH flow the interface between the up-going and down-going flows is vertical and straight; however, in helical flow the interface is twisted. The interface looks like what one would get if a long strip of paper is held at one end and the other end is turned through many turns; going along one edge of the strip one would trace an helix. Thus the two flows (up and down) take helical paths with a common (twisted) interface. In most cases we observe some mixing between the fluids in the two streams. Apparently the HAH flow is unstable above some (yet undetermined) critical Rayleigh number and the instability leads to helical flow.

Unsteady-laminar flow

In the 9.85 mm and 19.85 diameter tubes (i.e. at still higher Rayleigh numbers) we observe the flow to be unsteady and three dimensional, but laminar (Figures 5 and 6). There is no clear demarcation between the up-going and down-going flows, and there is a lot of mixing between the two. A typical mixing event involves collision of a downward going mass of fluid with a upward going mass of fluid, often leading to shear layers which go unstable with the formation of vortices. One also sees mushroom type structures (see Figure 5). The eddies seem to scale with the diameter of the tube. The flow is chaotic, but atleast in the 9.85 mm dia tube the flow is not turbulent: a range of scales, characteristic of turbulent flows is not present.

Figure 5. LIF picture showing unsteady-laminar convection. Note the mushroom structure. Tube diameter = 9.85 mm; concentration difference = 0.025 g/cc.

Figure 6. LIF picture showing unsteady-laminar convection. Tube diameter = 19.85 mm; Tube length = 300 mm; concentration difference = 0.025 g/cc.

Figure 7. LIF picture showing turbulent convection. Note the small length scales of mixing. Tube diameter = 37 mm; concentration difference = 0.025 g/cc.

Turbulent flow

What appears to be a truly turbulent flow is observed in the 36.85 mm diameter tube (Figure 7). Like in the 9.85 mm and 19.85 diameter tubes, the flow is chaotic and three dimensional. We observe collisions of fluid masses moving in opposing directions, and the formation and breakup of shear layers. During these interactions large interfacial areas are created greatly enhancing the mixing between the heavier and lighter fluids. Also because of collisions we can have instances when heavier masses of fluid move up instead of down, and similarly instances when lighter fluid masses go down. Both mixing and flow direction reversal contribute to reduction of flux, or in other words to slowing down of the experiment.

Flux relations

The flux times the tube cross sectional area, $-\overline{c\omega}A_p$, determines how fast the top tank depletes salt, or equivalently how fast the bottom tank accumulates salt. A large flux is obtained if all the down-going fluid ($w < 0$) has higher density ($c > 0$) (similarly when $w > 0$, c is < 0), and in addition if $|w|$ and $|c|$ are as large as possible. The maximum possible c is ΔC, when all the down-going fluid is pure top tank fluid and all the up-going fluid is pure bottom tank fluid; there is no mixing of the two in the tube. The maximum possible velocity is probably what is obtained by assuming half-and-half laminar flow, and whose solution is given below. Flux can be reduced due to two reasons. One, mixing between down-going and up-going fluids reduces the values of both c and w; two, heavier fluid moving down, or vice versa, reduces the correlation.

A trivial case is when there is no flow and the salt transfer is just by molecular diffusion; then flux is given by $F = \alpha\Delta C/l$. Stability analysis[4] shows that when the tube is thin enough or density difference small enough, or more precisely the gradient Rayleigh number $Ra_G < 1087$, there is no flow. (This analysis is for a density increasing linearly with height.) We never observed a no-flow case in any of our experiments as the Rayleigh number was above the critical value, except perhaps towards the end of an experiment when the density differences were too low to be measured by our instrumentation.

Next we derive expressions for the flux of salt in the vertical tube for two cases: (i) laminar half-and-half flow of immiscible fluids and (ii) turbulent convection.

Laminar HAH flow of immiscible fluids

Consider fully developed parallel flow in the vertical tube. We assume the heavier fluid (density = ρ_T) is going down in one half of the tube, say $\pi > \theta \geq 0$, and the lighter fluid (density = ρ_B) is going up in the other half, $2\pi > \theta \geq \pi$. Fluids in the two streams have same kinematic viscosity and are immiscible (equivalent to saying diffusivity of salt is zero). With U_r, $U_\theta = 0$ (parallel flow) and d/dz = 0 (fully developed flow), the Navier–Stokes equations simplify to

$$\frac{\partial p}{\partial r} = 0, \quad \frac{\partial p}{\partial \theta} = 0$$

in the r and θ directions, and

$$0 = -\frac{\partial p}{\partial z} - \rho g + \rho\nu\nabla^2 W,$$

is the z direction, where ∇^2 is the Laplacian operator in the $r - \theta$ plane. The boundary conditions are zero velocity at the wall ($r = d/2$) and at the interface ($\theta = 0$, $\theta = \pi$).

From a control-volume momentum balance, $-dp/dz = \rho_0 g$, where $\rho_0 = (\rho_T + \rho_B)/2$. Then the equation in the z direction, $0 = -(\rho - \rho_0)/\rho_0 + \nu\nabla^2 W$, which written separately for the upward going and downward going fluids becomes

$$\nu\nabla^2 W = -\frac{\Delta C}{2\rho_B} g \quad \text{(upward)}$$

$$\nu\nabla^2 W = \frac{\Delta C}{2\rho_T} g \quad \text{(downward)}.$$

To ensure symmetry we assume $(\Delta C/\rho_0) \ll 1$ and replace ρ_B and ρ_T by ρ_0 in the denominators on the right hand sides of the above equations.

Solution is same as that of a fully developed flow in pipe with a semi-circular cross section driven by a constant pressure gradient, but with the pressure gradient replaced by $g\Delta C$. The solution[5] gives the average velocity in each half of the tube as

$$\overline{W} = 0.0372\,l(d/2)^2 \frac{\Delta C}{\rho\nu} g\,.$$

The flux $(-\overline{wc}) = \Delta C\overline{W}/2$ is given by

$$F_l = 0.0059 \frac{d^2(\Delta C)^2}{\rho\nu} g, \tag{3}$$

where subscript l represents laminar flow. The relation shows the dependence of flux on various parameters and interestingly no dependence on the tube length.

In an experiment, even when the flow is HAH, because of diffusion of salt we would expect the flux to be lower than the theoretical value; the scaling will also probably change if diffusion is included. However eq. (3) gives a theoretical maximum value and can be used to non-dimensionalize experimental flux values.

Turbulent flow

We make certain assumptions based on dimensional and physical arguments to arrive at a relation for flux when the flow is turbulent. Clearly other expressions can be obtained by making different assumptions.

We assume fully developed flow – the flow is identical (in an average sense) at different Z locations, and we assume the flow is steady (again in an average sense). The first assumption will be valid if the tube is sufficiently long ($(l/d) \gg 1$) and we are far enough away from the two ends; how long and how far will have to be determined from experiments. A similar situation arises in fully developed, pressure-gradient driven turbulent pipe flow. In that case, fully developed flow is achieved about 20–50 diameters from the entrance, and in the length of the pipe where the flow is fully developed, profiles of mean velocity and, for example, profiles of the mean turbulent stresses do not change with axial distance; and the axial pressure gradient is constant.

From the fully developed flow condition we have the mean density (or concentration) gradient $d\langle C\rangle/dz$ = constant. (For the turbulent flow we use $\langle\ \rangle$ to denote time average, and prime to denote deviation from the time average.) Like the pressure gradient in the case of the pipe flow, we have the density gradient as the driving force in the vertical-tube convection flow. The independent parameters are then $d\langle C\rangle/dz$, ρ, g, and d. Viscosity and diffusivity are not considered, an usual assumption in turbulent flow.

In the vertical-tube convection case we have seen there is no mean flow, i.e. $\overline{W} = 0$. From flow visualization we have seen that when the flow is turbulent there are no two clear streams of upgoing and downgoing fluids. Thus the relevant parameters describing the flow are the flux $-\langle \omega' c' \rangle$, and means of the squares of fluctuating velocities ($\langle u_r'^2 \rangle$, $\langle u_\theta'^2 \rangle$ and $\langle w'^2 \rangle$) and of concentration fluctuations ($\langle c'^2 \rangle$). Prime denotes deviation from the time average.

We assume the flux to be proportional to the product of a velocity scale (say W_{turb}) and a concentration scale (say C_{turb}). These quantities may be thought of as associated with a typical fluid mass or an eddy: say a heavier fluid mass with an excess density over the ambient = C_{turb}, and moving down with a velocity W_{turb}. From the above list of independent parameters we get

$$C_{\text{turb}} = \frac{\mathrm{d}\langle C \rangle}{\mathrm{d}z} d.$$

The velocity scale can be obtained as the velocity attained by the fluid mass during free fall over some distance (a mixing length). We assume the mixing length scales as the diameter. Thus

$$W_{\text{turb}} = \left(\frac{C_{\text{turb}} g d}{\rho} \right)^{1/2} = \left(\frac{\mathrm{d}\langle C \rangle}{\mathrm{d}z} \frac{g d^2}{\rho} \right)^{1/2}.$$

Then the relation for turbulent flux is

$$F_{\text{T}} = K_{\text{T}} \left(\frac{\mathrm{d}\langle C \rangle}{\mathrm{d}z} \right)^{3/2} \left(\frac{g}{\rho} \right)^{1/2} d^2,$$

where K_{T} is a constant. Neglecting the end effects we can write $\mathrm{d}\langle C \rangle / \mathrm{d}z = (C_{\text{T}} - C_{\text{B}})/l = \Delta C / l$. Then the above expression becomes

$$F_{\text{T}} = K_{\text{T}} \frac{\Delta C^{3/2} g^{1/2} d^2}{\rho^{1/2} k^{3/2}}. \tag{4}$$

Note that the dependence on the various parameters is different from that obtained in the laminar HAH flow case (eq. (3)). In contrast to the laminar flow case, in the turbulent flow a length dependence ($= l^{-3/2}$) is present and viscosity does not enter the picture.

Experimental flux results

We compare the experimentally obtained flux of salt with the theoretically predicted flux. As mentioned earlier, from the measured salt concentration in the top tank fluid we calculate the density difference (ΔC) using relations (1) and the flux (F) using relation (2).

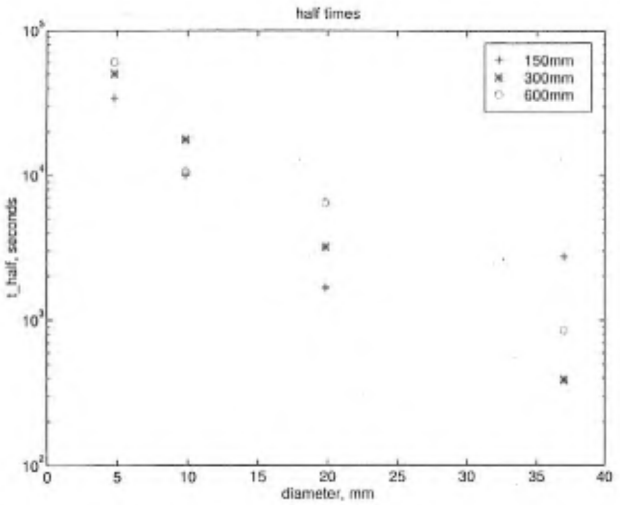

Figure 8. The half-times in the experiments with different diameter and different length tubes.

First, to give an idea of the durations of the experiments. Figure 8 shows the half-times obtained in all the experiments we have conducted. Faster mixing is obtained as the tube diameter increases, and for a given diameter the mixing is slower for a longer tube. The half time ranges from about 400 s in the case of the 36.85 mm diameter, 150 mm long tube to about 6×10^4 seconds in the case of the 4.8 mm diameter, 600 mm long tube.

Figure 9 shows for the 4.85 mm diameter cases the flux normalized by F_J (the theoretical flux for laminar HAH flow of immiscible fluids) vs Rayleigh number based on diameter. Recall in this diameter tube the flow is laminar helical type. The normalized flux values are only about 0.02 to 0.04. Clearly diffusion and mixing results in flux values much lower than theoretical values. The normalized flux value is even lower for convection in the larger diameter tubes: about 0.005 for 9.85 mm diameter tubes, and 0.001 for 36.85 mm diameter tubes.

At the other extreme is turbulent flow. We had discussed that the flow in the 36.85 mm diameter tubes appeared to be turbulent visually. We can check whether the flux in these tubes scales as predicted by the relation (4), which is for turbulent flow. Figure 10 shows, for the 300 mm and 600 mm tube lengths, the normalized flux (F/F_{T}) data plotted versus the Rayleigh number based on the diameter (K_{T} has been taken to be unity in calculating F_{T} in the plot). The data for the two diameters collapse to a reasonable extent. The normalized flux appear to be nearly constant with Rayleigh number. The constant K_{T}, in eq. (4), from the plot is about 0.5. More experiments covering a wider range of Rayleigh numbers are needed to validate and extend these results.

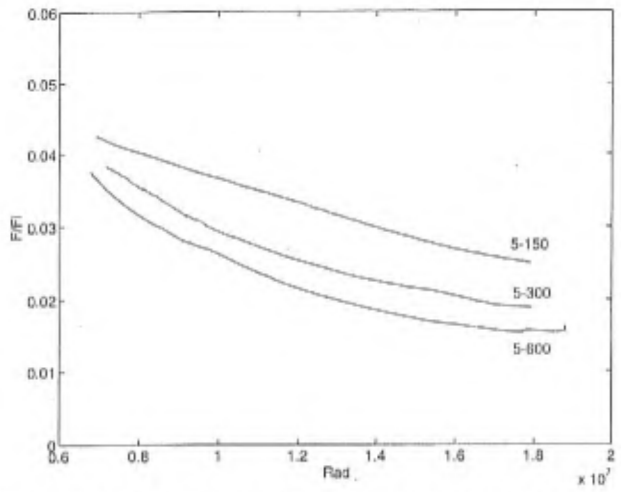

Figure 9. Plot of flux normalized by theoretical laminar flux vs Rayleigh number in the case of 4.85 mm diameter tube.

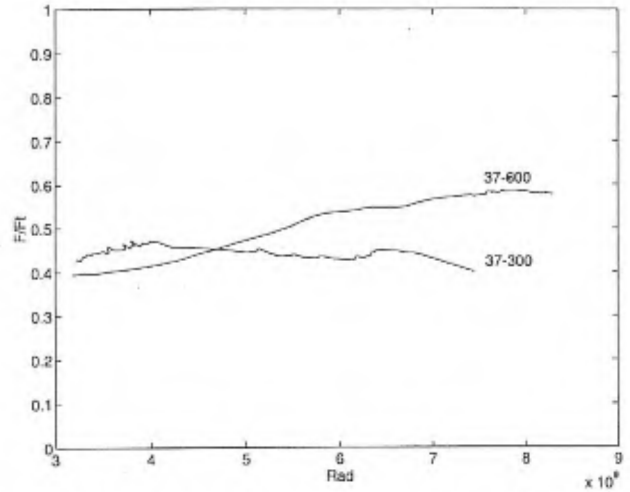

Figure 10. Plot of flux normalized by theoretical turbulent flux vs Rayleigh number in the case of 36.85 mm diameter tube.

Conclusions

We have presented preliminary results on natural convection in a vertical tube. More work is needed to resolve a number of issues; two main ones are listed below:

(i) We have given the solution for laminar HAH flow of fluids with zero diffusivity ($Pr \to \infty$). We need to solve for finite Prandtl numbers to realistically compare data from experiments.

(ii) We need to precisely determine the values of the transition Rayleigh numbers, when the flow switches from one type of flow to the other.

But what we think is interesting is the turbulent flow. It appears to be different from the other types of turbulent flow which we are familiar with: free shear flows like jets, wakes, plumes, or wall bounded flows like turbulent flow in a pipe, flow on a heated vertical wall. We have in the vertical-tube convection case a buoyancy-driven turbulent flow with zero mean flow and zero mean shear. Here mean refers to time average. Thus at any spatial point in the flow the time averages of the vertical velocity and of the shear are zero. The flow is homogeneous in the vertical direction and appears to be nearly homogeneous in the horizontal direction; because of zero mean flow the (side) wall seems to just 'contain' the flow, and does not have the overwhelming influence it has, for example, in the pressure-driven turbulent pipe flow. Besides the fluid properties and gravity, the only parameters are tube diameter and the forcing term, the density gradient.

This flow has relevance to turbulent R–B convection and during the later stages of Rayleigh–Taylor instability. In R–B convection the flow away from the walls (in the core) is similar to what is obtained in the vertical-tube convection. In R–B convection, it is well known that the wall predominantly determines the dynamics, but an issue of current interest is the interaction between the wall and core flows[5,6]. An understanding of this interaction may help resolve the controversy regarding the exponent in the Nusselt number–Rayleigh number correlation[3]. The vertical-tube convection can shed light on the turbulent mixing during Rayleigh–Taylor instability, where, as in the tube convection case, a simultaneous motion of heavy and light fluids is obtained. Finally, the vertical-tube turbulent convection may be similar to the decaying homogeneous buoyancy-driven turbulence studied by Batchelor *et al.*[8], using numerical simulation, except that, in our case the turbulence is non-decaying.

1. Turner, J. S., *Buoyancy Effects in Fluids*, Cambridge, 1972.
2. Dalziel, S. B., Linden, P. F. and Youngs, D. L., *J. Fluid Mech.*, 1999, **399**, 1–48.
3. Niamela, J. J., Skrbek, L., Sreenivasan, K. R. and Donnelly, R. J., *Nature*, 2000, **404**, 837–840.
4. Batchelor, G. K. and Nitsche, J. M., *J. Fluid Mech.*, 1993, **252**, 419–448.
5. White, F. M., McGraw Hill, 1991.
6. Theerthan, S. A. and Arakeri, J. H., *J. Fluid Mech.*, 1998, **373**, 221.
7. Theerthan, S. A. and Arakeri, J. H., *Phys. Fluids*, 2000, **12**, 884.
8. Batchelor, G. K., Canuto, V. M. and Chasnov, J. R., *J. Fluid Mech.*, 1991, **235**, 349–378.

ACKNOWLEDGEMENT. J.H.A. acknowledges the travel support from the Third World Academy of Sciences, and thanks the people at CIE who made the stay in Mexico during March to June, 1998 a pleasant one. We thank Murali Cholemari for help in manuscript preparation.